Laser tunneling from aligned molecules

C T L Smeenk,[1] L Arissian,[2] A V Sokolov,[3] M Spanner,[1] K F Lee,[1,3] A Staudte,[1] D M Villeneuve,[1] and P B Corkum[1]

[1] *JASLab, University of Ottawa and National Research Council, 100 Sussex Drive, Ottawa, Canada*
[2] *Department of Electrical and Computer Engineering, University of New Mexico, Albuquerque, USA*
[3] *Department of Physics, Texas A & M University, College Station, USA*

We study multi-photon ionization from N_2, O_2 and benzene using circularly polarized light. By examining molecular frame photo-electron angular distributions, we illustrate how multi-photon ionization acts a momentum-selective probe of the local electron density in the Dyson orbitals for these molecules. We find good agreement with calculations based on a tunneling model and including saturation effects.

Ionization of atoms, molecules, and solids by strong infrared laser fields is a common approach to control and study ultrafast phenomena [1, 2]. Light-matter interaction in this limit is often modelled as tunneling. For the rare gas atoms tunneling accurately predicts the ionization rate over many orders of magnitude [3]. Tunneling models place additional limits on the continuum wavefunction of the photo-electron [4], but only recently have experiments begun to test these more subtle predictions [5–7]. Analytical models of atomic ionization suggest that the momentum distribution of the bound electron is imprinted onto the continuum wavefunction [8]. However experiment, simulations, and quantitative theory all show the lateral momentum distribution exceeds the analytical width by $10-15\%$ [5, 9, 10]. Nonetheless, both experiment and calculations illustrate that multi- photon ionization transfers information from the bound orbital to the continuum.

Work with small molecules is more qualitative. Experiments show that orbital information, especially the location of nodal planes, is transferred to the ionizing wavepacket [11–13]. The wavepacket structure that emerges is important for many applications like high-harmonic spectroscopy [14–16], laser-induced electron diffraction and holography [17–20], and orbital tomography [21, 22]. Despite its importance for ultrafast science, there are few quantitative tests on strong field ionization of molecules. In this paper we experimentally study three different molecules – N_2, O_2 and C_6H_6 – to test how well theoretical concepts from tunneling of atoms transfer to molecular strong field ionization.

We will show that, for the three molecules we study, the saturation intensity depends on the molecular alignment. In the cases of O_2 and C_6H_6 the difference is consistent with the intuitive predictions made by analytical theory [8], however, in N_2 it is not. The deviation in N_2 is consistent with prior experimental work [23] and suggests modifications to the filtered orbital concept [8, 11]. We also find the lateral momentum distribution from the three molecules is consistent with the values measured in atoms at similar laser parameters [5].

Our experimental approach is influenced by work on atoms. We use circularly polarized light at 800 nm to ensure re-collision is essentially eliminated. Thus, the momentum along the laser propagation axis (z) is the quantum uncertainty of the electron when it departs the tunneling barrier. In addition, the photo-electron momentum in the plane of polarization allows us to determine the laser field strength at ionization [24].

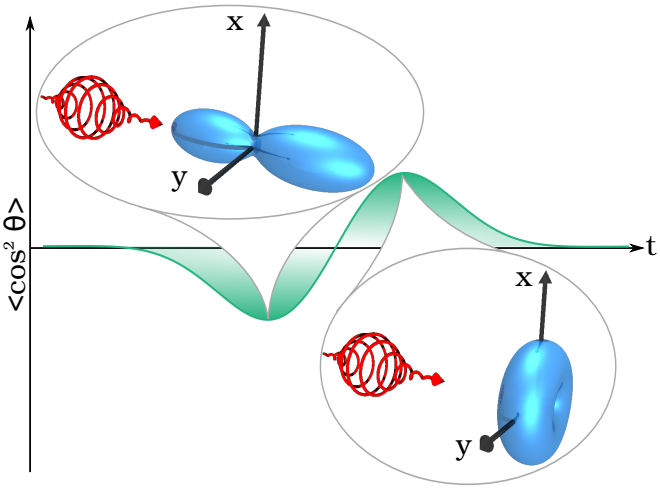

FIG. 1. Concept of the experiment using circularly polarized pump & probe laser pulses. The full revival of N_2 is sketched as the green curve. Just prior to the revival, the molecular alignment distribution, sketched in blue, is parallel to the propagation axis (k-alignment; inset upper left). A circularly polarized probe pulse shown in red singly ionizes the k-aligned molecules. For a slightly longer pump-probe delay the molecular alignment is confined to the plane of polarization (inset lower right). We record photo-electron spectra from single ionization under both alignment conditions. See the text for a discussion of the alignment revivals in O_2 and benzene.

We use field-free non-adiabatic alignment to control the molecular alignment in the lab frame [25]. This makes our approach applicable to neutral molecules without a permanent dipole but it imposes a cost of imperfect control over the molecular frame. To handle this limitation we adopt the method of normalized differences [11]. This has the added advantage of removing the need to calibrate the detector response. Additionally, we have used a circularly polarized pump pulse to align the molecules. In a circularly polarized aligning pulse, the most polariz-

able axis of the molecule receives a torque into the plane of polarization (xy – see Fig. 1). This creates a rotational wavepacket that re-aligns to the plane of polarization every full revival period T_R. For a linear molecule, just before the full revival the internuclear axis first aligns along the direction of laser propagation, z (Fig. 1; inset left). We call this "k-alignment". The molecules continue to rotate and a short time later the internuclear axis is aligned with the plane of polarization (Fig. 1; inset right). We call this "aplanement". We recorded photo-electron spectra under k-alignment and aplanement for all three molecules.

Experimentally, we use 40 fs pulses at 800 nm and in the range $4 \times 10^{13} - 4 \times 10^{14}$ W/cm^2. The pulses are split into a pump and probe using a beam-splitter with variable attenuation control in each arm. The circularly polarized pump pulse was stretched to $\sim$ 60 fs for the small molecules (N_2 and O_2) or 250 fs for benzene. The pump laser pulse is focused by an $f/25$ parabolic mirror onto a pulsed, supersonic gas jet (Even-Lavie valve) operating at 1 kHz. The jet temperature was estimated to be 5 K. By exploding the molecules and measuring the momentum distributions from N^{2+} and O^{2+} fragments, we measured the degree of alignment $\langle \cos^2 \theta \rangle = 0.7$ for N_2 and O_2. For benzene we used the proton momentum distribution measured with respect to the k-axis to observe aplanement and anti-aplanement.

We use a circularly polarized probe pulse to singly ionize the aligned or aplaned molecules. The probe was focused onto the sample of aligned molecules with the same parabolic mirror at $f/12.5$. The timing of the probe was precisely controlled by an automated delay stage. In N_2 we used the half revival (aplanement: 4.07 ps, k-alignment: 4.40 ps). For O_2 we used the quarter revival for aplanement (2.90 ps) and three-quarter revival for k-alignment (8.68 ps). Lastly, for benzene we used the full revival for anti-aplanement (87.2 ps) and aplanement (88.8 ps). In the benzene case the distributions sketched in blue in Fig. 1 correspond to the vector normal to the plane containing the carbon and hydrogen nuclei. Aplanement of benzene corresponds to aligning the normal vector along the k-axis (Fig. 1 left). Anti-aplanement of benzene corresponds to the normal vector de-localized in the plane of polarization (Fig. 1 right). (Since we used the full revival for benzene, the timing of the molecular aplanement and anti-aplanement is switched with respect to the half revival shown in Fig. 1.)

The photo-electron spectra were recorded by a velocity map imaging spectrometer (VMI) [26] read out by a CCD camera (DVC 1312M) and stored on a desktop computer. The spectra were corrected for dark noise in the camera by subtracting an image taken with the laser pulses blocked. Because of the large inhomogeneous electric field in the spectrometer ($\approx$ 1 kV/cm) and the small mass of electrons, each measured spectrum is a two-dimensional projection of the 3D molecular frame momentum distribution. Each measurement contains $\sim 2 \times 10^7$ detected electrons acquired at a rate of 1.2 electrons/laser pulse.

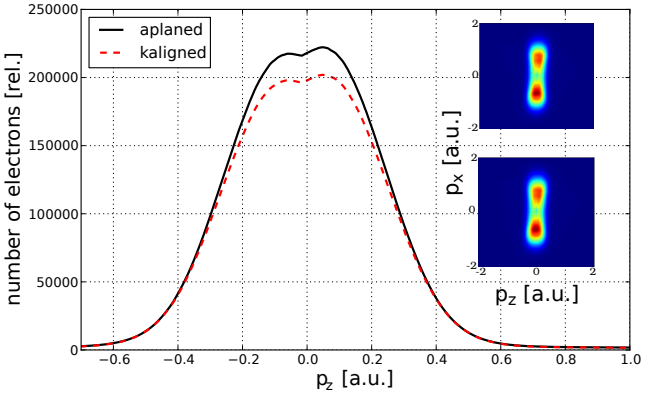

FIG. 2. Raw lateral momentum distributions for aplaned and k-aligned O_2 integrated over the plane of polarization. k-aligned O_2 shows ionization suppression by about 7%. The dip at $p_z = 0$ is due to detector inhomogeneity. Inset: Raw 2D photo-electron distributions for aplaned (upper) and k-aligned (lower) O_2.

An example of the measured raw photo-electron momentum distributions from O_2 at aplanement and k-alignment are shown in Fig. 2. The raw distributions are largely a reflection of the strong limits on the electron momentum imposed by the shape of the potential barrier. Along the z axis the exponential fall off in ionization probability is due to the increasing tunnel barrier in the lateral direction [5]. Tunneling theory predicts the lateral photo-electron distribution takes the form (in atomic units) [4, 8]

$$|\psi(p_\perp)|^2 \propto \int \mathrm{d}p_\parallel \, |\psi_0|^2 \exp\left(-p_\perp^2 \frac{\sqrt{2I_p(\beta)}}{E}\right) \qquad (1)$$

where $p_\perp$ is the electron momentum perpendicular to the laser field, ψ_0 is the bound momentum distribution and $I_p(\beta)$ is the Stark shifted ionization potential which depends on β, the angle between the laser polarization vector and the major and minor polarizability axes [13, 27, 28]. In the plane of polarization (xy) the photo-electron drift momentum $p = E(t_i)/\omega$ where $E(t_i)$ is the laser field strength at the time of ionization and ω is the laser angular frequency.

The qualitative features in Fig. 2 are largely the same for k-aligned and aplaned molecules. This is a reflection of imperfect alignment. However, there is 7% less signal from k-aligned O_2 compared to aplaned molecules. This is due to suppressed ionization [29]. From N_2 and benzene we also observed suppressed ionization from the k-aligned or aplaned molecules respectively. The suppression was 7% was N_2 and 5% from benzene. Since we will use normalized differences the spectra are not corrected for the reduced sensitivity of our micro-channel

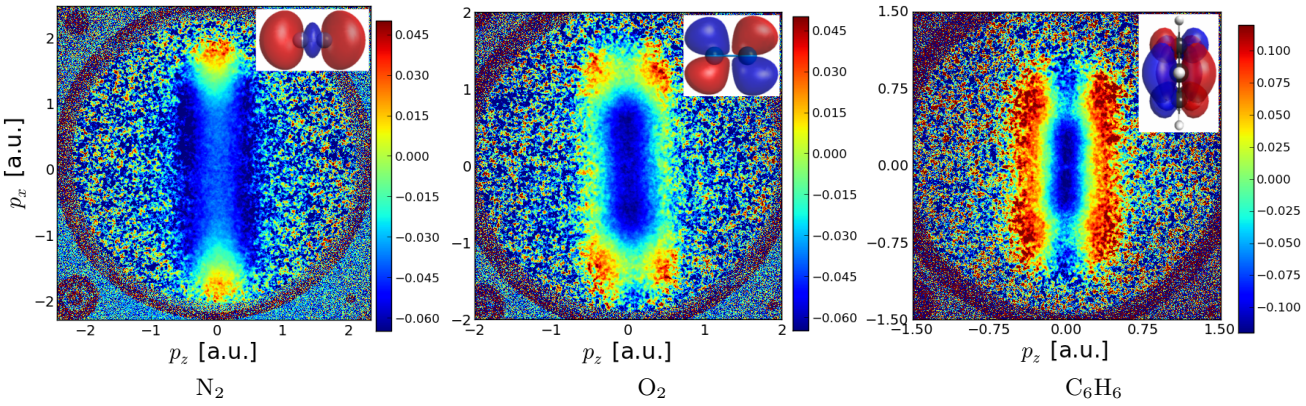

FIG. 3. Experimental normalized difference spectra for the three molecules. Normalized difference is $(a-b)/(a+b)$ where a is the photo-electron spectrum measured at k-alignment (benzene: aplanement) and b at aplanement (benzene: anti-aplanement). Inset shows the Dyson orbitals of each molecule. **Left:** N_2 at 4.5×10^{14} W/cm^2. **Centre:** O_2 at 2.7×10^{14} W/cm^2. **Right:** Benzene at 4.0×10^{13} W/cm^2.

plate detector at $p=0$. This reduced sensitivity is responsible for the on axis minimum and the asymmetry in the raw spectra in Fig. 2. By using normalized differences, the detector response is calibrated out.

While this raw width of the lateral distribution from the three molecules is largely consistent with the values measured in atoms [5], we are able to precisely compare the relative width of the lateral distribution for k-aligned vs. aplaned molecules. In O_2 the k-aligned distribution is 2.3% wider ($1/e$ half width) than the aplaned distribution, however, in benzene the aplaned distribution is 12.3% wider. In N_2 the aplaned spectrum was 1.3% wider than the k-aligned spectrum.

To observe more clearly the features of the bound orbital in the tunneled photo-electron distributions, we process the measured 2D spectra by taking normalized difference, $ND=(a-b)/(a+b)$ where a and b are the k-aligned (benzene: aplaned) and aplaned (benzene: anti-apalaned) distributions respectively. By subtracting and dividing two distributions we can partially remove the effect of the large contribution from the tunnel barrier itself and observe the small modulations due to different orientations of the bound state wave-function ψ_0. This also removes the inhomogeneous detection sensitivity.

In Fig. 3 we show examples of the normalized difference spectra for N_2, O_2 and benzene. Each spectrum shows evidence of the symmetry of the Dyson orbital. The Dyson orbital of N_2 has maximum electron density at $p_z\approx0$. Additionally, ionization perpendicular to the molecular axis (from k-aligned molecules) has a lower rate than parallel to the molecular axis (aplaned molecules) [23]. As we will show, this creates the bright red regions at larger longitudinal momentum ($p_x\approx1.8$). As one looks at larger lateral momenta ($|p_z|>0.8$) the ionization probability drops by 10^{-4} and the signal is lost to experimental noise. This is the effect of the tunnel barrier.

In the O_2 spectra, the k-aligned molecules have minimum electron density along the polarization axis. Ionization along $p_z\approx0$ is therefore suppressed compared to molecules aligned in the plane of polarization. As we will show later, this also means the k-aligned molecules will saturate later in the laser pulse when the laser field strength is larger. These two combined effects produce the four bright corners on the edges of the O_2 spectra (Fig. 3 center). In benzene there is a nodal plane in the Dyson orbital along the molecular plane. The difference between the aplaned and anti-aplaned molecules creates the regions of positive signal at large lateral momentum ($|p_z|>0.3$) shown in red in Fig. 3 (right column). This corresponds to the larger electron density in the Dyson orbital of aplaned benzene. In Fig. 3 there is a qualitative transition between molecules with maximum electron density in the low lateral momentum region of the tunnel (N_2) and those with minimum electron density (O_2, C_6H_6).

To test the consistency of our observations with the tunneling model, we developed a semi-classical numerical simulation of tunnel ionization from a Dyson orbital in circularly polarized light. To begin, we calculate an ab-initio Dyson orbital and Fourier transform it to make a 3D momentum-space orbital $\psi(\boldsymbol{p})$. The momentum space orbital is rotated into the desired orientation in the lab frame. For the anti-aplanement of linear molecules, the molecular axis lies along p_z. To calculate an aplaned distribution we integrate over 30 angles in the plane of polarization (xy).

The laser field is given by $\boldsymbol{E}(t) = E\ e^{-2\ln2t^2/\tau^2}\ [\sin\omega t\ \hat{\imath}-\cos\omega t\ \hat{\jmath}]$ where τ is the FWHM pulse duration and $\hat{\imath}$, $\hat{\jmath}$ are unit vectors in the plane of polarization. At each phase of the laser field $0\le\omega t<2\pi$ the momentum distribution is further rotated with respect to the polarization of the ionizing field. This makes two assumptions: (1) $\psi(\boldsymbol{p})$ is fixed

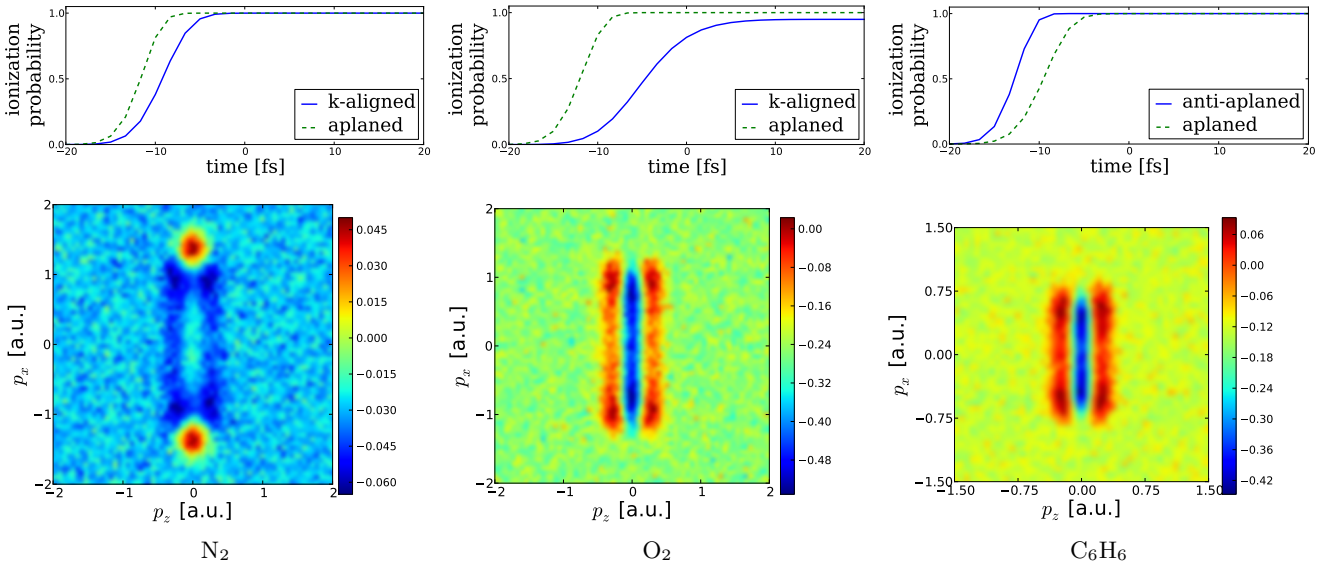

FIG. 4. **Upper row:** Ionization probability as a function of time in a circularly polarized 40 fs pulse for k-aligned (anti-aplaned) and aplaned molecules. **Lower row:** Calculated normalized difference spectra $(a-b)/(a+b)$ where a is the photo-electron spectrum measured at k-alignment (benzene: aplanement) and b at aplanement (benzene: anti-aplanement). **Left:** N_2 at 4.5×10^{14} W/cm^2. **Centre:** O_2 at 2.7×10^{14} W/cm^2. **Right:** Benzene at 4.0×10^{13} W/cm^2. 1% Gaussian noise was added to each calculated spectrum prior to processing.

with respect to the molecular frame, (2) the electron wave-function adiabatically adjusts to the rotating laser field. To calculate the tunneled distribution at a given phase, we use Eq. 1 to calculate the lateral distribution. The lateral distribution is then mapped onto a torus using the classical drift momentum: $\boldsymbol{p} = \frac{E}{\omega}e^{-2\ln 2t_i^2/\tau^2}\ [\cos\omega t_i\ \hat{\imath} + \sin\omega t_i\ \hat{\jmath}]$ where t_i is the time of ionization. Integrating over each phase of the circularly polarized pulse creates a 3D distribution for a particular alignment of the molecule in the lab frame.

To study the effect of saturation in the resulting photo-electron distributions, we track the remaining population in the neutral molecule. To calculate the alignment dependent tunneling rate, we use a modified version of a molecular tunneling theory [30]. We write the instantaneous ionization rate as

$$W\left(E(t),\beta\right) = W_{ADK}\left(E(t), I_p(\beta)\right)\cdot\alpha(\beta) \times \int \mathrm{d}p_\perp \mathrm{d}p_\parallel \left|\psi_0(\boldsymbol{p},\beta)\right|^2 \exp\left(-p_\perp^2\frac{\sqrt{2I_p(\beta)}}{E(t)}\right) \quad (2)$$

where $W_{ADK}(E)$ is the atomic tunnel ionization rate depending on E and $I_p(\beta)$ [2], $\alpha(\beta)$ is a free scalar parameter and the third factor includes the effect of the bound momentum orbital, ψ_0. Eq. 2 is similar in spirit to many theories on multi-photon ionization of molecules which split the rate into an atomic tunneling part and a geometrical part [29–31]. For the π orbitals in O_2 and benzene $\alpha(\beta) =$ const. and Eq. 2 predicts the angle dependent ionization rate is suppressed along a nodal axis. This is consistent with experiment [12, 13].

In the case of N_2, however, we require $\alpha(0) \approx 4\alpha(\pi/2)$ to predict the suppression of ionization perpendicular to the molecular axis [23]. This is true even when including angle dependent Stark shifts.

The ionization probability from the Dyson orbital is given by $P(t) = 1 - \exp\left[-\int_{-\infty}^{t} W(E(t'),\beta)\mathrm{d}t'\right]$ and the instantaneous ionization yield is $\mathrm{d}P/\mathrm{d}t$. We use the instantaneous yield to weight the contribution from a particular alignment angle as a function of time in the 40 fs pulse. At each time step we average the yield over all alignments present in the molecular distribution to calculate the net yield. From Eq. 2 it is clear the yield depends on the alignment of the bound orbital with respect to the polarization axis, in addition to the length of the tunnel barrier $\approx I_p/E$. The yield also depends on the remaining population in the Dyson orbital. The result is shown in the upper row of Fig. 4.

To compare our tunneling calculations to the experimental distributions we apply the algorithm to the Dyson orbitals of N_2, O_2 and benzene. In each case, the orbitals were rotated to create either a k-aligned/anti-aplaned or aplaned set of molecular alignments. We used the experimental intensity values to calculate the tunneled electron distributions and scaled the total number of electrons in each calculated spectrum according to the experimental values. We did not include alignment distributions out of the plane of polarization because we found these only change the contrast in the calculated spectra and do not yield new qualitative features. To compare with Fig. 3 we then created the normalized difference of the k-aligned/anti-aplaned vs. aplaned spectra. The result is

shown in Fig. 4.

Figure 4 shows the role of saturation in the calculation. For N_2 (left) and O_2 (centre) the ionization rate from k-aligned molecules is lower than for the aplaned molecules. This means that more population survives in the neutral k-aligned molecules later on in the pulse when the laser field is larger. Consequently the photo-electron distribution is shifted to slightly larger drift momentum $p = E(t_i)/\omega$. This is the reason for the four bright red features on the corners of the O_2 distribution (centre column in Fig. 3 and 4). In our calculations saturation also plays a role in creating the bright red regions at large longitudinal momentum ($|p_x| \approx 1.8$) in the N_2 distribution. This is again a consequence of the neutral k-aligned molecules surviving later into the pulse when the laser field is larger. For benzene, the nodal plane along the molecular axis means that the aplaned molecules have a lower ionization rate and hence saturate later in the pulse as verified in Fig. 4 right. The combination of the large electron density at non-zero lateral momentum, and shorter tunnel barrier around the maximum of the pulse envelope produces the bright red vertical stripes along the sides of the benzene differences spectra (Figs. 3, 4).

The agreement between Figs. 3 and 4 illustrates how tunneling probes the local electron density in a static molecular orbital. In k-aligned O_2 and aplaned benzene the Dyson orbital has a minimum in the electron density along the polarization axis. In this case we observe that bright positive regions in the differences and normalized differences appear at larger longitudinal momentum, and for non-zero lateral momentum ($|p_z| > 0.3$). Because of the absence of electron density along the polarization axis both the total ionization rate and the photo-electron amplitude at $p_z = 0$ are suppressed. In k-aligned N_2, the Dyson orbital has maximum electron density at zero lateral momentum. We observe ionization from those molecules is enhanced along the polarization axis and at large longitudinal momentum.

The transition from a local minimum to maximum amplitude along the tunneling axis is potentially a useful technique for detecting motion of molecular electronic wavepackets. If several ionic states are populated by a pump pulse, the ensuing electronic wavepacket could be probed in the molecular frame using tunnelling by a few-cycle laser field [32]. Modulations in the low lateral momentum region of the bound electron density would then be imprinted onto the tunnelled photo-electron distribution, much like we have shown here for static orbitals.

By recording MFPADs under different molecular alignment conditions, we have shown how the selectivity of laser tunneling is imprinted onto the photo-electron spectrum. Tunneling acts as a momentum selective filter that is sensitive to the local electron density. Technical improvements in molecular cooling, alignment and orientation will lead to improvements in the resolution of the tunneling spectra, much like vibrational isolation is a prerequisite for high resolution STM. This could be exploited in future studies on molecular electronic wavepackets [33, 34].

[1] F Krausz and M Ivanov. *Rev. Mod. Phys.*, 81(1):163, 2009.
[2] Z Chang. *Fundamentals of Attosecond Optics*. CRC Press, 2011.
[3] B Walker, et al. *Phys. Rev. Lett.*, 73(9):1227, 1994.
[4] N B Delone and V P Krainov. *JOSA B*, 8(6):1207, 1991.
[5] L Arissian, et al. *Phys. Rev. Lett.*, 105(13):133002, 2010.
[6] C T L Smeenk, et al. *Phys. Rev. Lett.*, 106:193002, 2011.
[7] A N Pfeiffer, et al. *Phys Rev Lett*, 109:083002, 2012.
[8] M Ivanov, M Spanner, and O Smirnova. *J Mod. Opt.*, 52(2 - 3):165, 2005.
[9] J Henkel, M Lein, V Engel, and I Dreissigacker. *Phys. Rev. A*, 85:021402, 2012.
[10] I Dreissigacker and M Lein. *Chem Phys*, 414(0):69 – 72, 2013.
[11] M Meckel, et al. *Science*, 320(5882):1478, 2008.
[12] H Akagi, et al. *Science*, 325(5946):1364, 2009.
[13] L Holmegaard, et al. *Nature Phys.*, 6:428, 2010.
[14] S. Baker, et al. *Science*, 312(5772):424, 2006.
[15] T Kanai, et al. *Phys. Rev. Lett.*, 98:153904, 2007.
[16] A Shiner, et al. *Nature Phys.*, 7:464, 2011.
[17] D. Ray, et al. *Phys. Rev. Lett.*, 100:143002, 2008.
[18] M Okunishi, et al. *Phys Rev Lett*, 100:143001, 2008.
[19] M Spanner, O Smirnova, P B Corkum, and M Ivanov. *J Phys B*, 37:L243, 2004.
[20] Y. Huismans, et al. *Science*, 331(6013):61–64, 2011.
[21] J. Itatani, et al. *Nature*, 432(7019):867–871, 2004.
[22] C. Vozzi, et al. *Nat Phys*, 7(10):822–826, 2011.
[23] I V Litvinyuk, et al. *Phys. Rev. Lett.*, 90:233003, 2003.
[24] C Smeenk, et al. *Opt. Exp.*, 19(10):9336, 2011.
[25] H Stapelfeldt and T Seideman. *Rev. Mod. Phys.*, 75:543, 2003.
[26] A Eppink and D Parker. *Rev. Sci. Instruments*, 68(9):3477, 1997.
[27] K J Miller. *J Am Chem Soc*, 112:8543, 1990.
[28] S M Smith, et al. *J Phys Chem A*, 108(50):11063–11072, 2004.
[29] J Muth-Böhm, A Becker, and F H M Faisal. *Phys Rev Lett*, 85:2280, 2000.
[30] R Murray, M Spanner, S Patchkovskii, and M Y Ivanov. *Phys Rev Lett*, 106:173001, 2011.
[31] X M Tong, Z X Zhao, and C D Lin. *Phys Rev A*, 66:033402, 2002.
[32] A Fleischer, et al. *Phys. Rev. Lett.*, 107:113003, 2011.
[33] J. Breidbach and L. S. Cederbaum. *J Chem Phys*, 118(9):3983–3996, 2003.
[34] F. Remacle and R. D. Levine. *PNAS*, 103(18):6793–6798, 2006.